Supporting Information

Tuning the optoelectronic properties for high-efficiency (>7.5%) all small molecule and fullerene-free solar cells.

Tuning the optoelectronic properties for high-efficiency (>7.5%) all small molecule and fullerene-free solar cells.

María Privado[a], Virginia Cuesta[a], Pilar de la Cruz[a], Mukhamed L. Keshtov[b], Ganesh D. Sharma,[c*] Fernando Langa[a,*]

[a] *Universidad de Castilla-La Mancha, Institute of Nanoscience, Nanotechnology and Molecular Materials (INAMOL), Campus de la Fábrica de Armas, Toledo, Spain. *e-mail: Fernando.Langa@uclm.es*

[b] *Institute of Organoelement Compounds of the Russian Academy of Sciences, Vavilova St., 28, 119991 Moscow, Russian Federation*

[c] *Department of Physics, LNM Institute of Information Technology (Deemed University), Jamdoli, Rupa ki Nagal, Jaipur (Raj.) 302031, India, *e-mail: gdsharma273@gmail.com and gdsharma@lnmiit.ac.in*

1. Experimental conditions.

Anhydrous solvents were dried by purification system Pure-Sov 400. Chromatographic purifications were performed using silica gel 60 Merk 230-400 mesh ASTM. Analytical thin-layer chromatography was performed using ALUGRAM ® SIL G/UV_{254} silica gel 60. Nuclear magnetic resonance ^{1}H NMR and ^{13}C NMR were performed using Bruker Innova 400 Hz. Chemical shifts (δ) values are denoted in ppm. Residual solvent peaks being used as the internal standard ($CHCl_3$; δ = 7.27 ppm). ^{13}C NMR chemical shifts are reported relative to the solvent residual peaks ($CDCl_3$, δ = 77.00 ppm). MALDI-TOF spectra were obtained in VOYAGER DETM STR spectrometry, using dithranol [1,8-dihydroxy-9(10H)-anthracenone] as matrix. Fourier transform infrared spectrophotometer (FT-IR) Thermo Nicolet AVATAR 370 was used with KBr method, in each case the most characteristic bands are indicated for each compound. Absorption spectra were performed on Shimadzu UV 3600 spectrophotometer. Solutions of different concentration were prepared in CH_2Cl_2, spectroscopy grade, with absorbance between 0.5 and 0.7 using a 1 cm UV cuvette. The TGA (heating rate of 10 ºC/min) and DSC analysis were done on a Mettler Toledo TGA/DSC Start^{e} System under nitrogen.

Electrochemical Measurements: Reduction (E_{red}) and oxidation potentials (E_{ox}) were measured by cyclic voltammetry with a potentiostat BAS CV50W in a conventional three-electrode cell equipped with a glassy carbon working electrode, a platinum wire counter electrode, and an $Ag/AgNO_3$ reference electrode at scan rate of 100 mV/s. The E_{red} and E_{ox} were expressed vs. Fc/Fc^+ used as external reference. In each case, the measurements were done in a deaerated solution containing 1 mM of a the sample compound in 0.1 M of $(n\text{-Bu})_4NClO_4$ in *o*-DCB:Acetonitrile (4:1) as an electrolyte solution.

Computational Details: Theoretical calculations were carried by using the Gaussian 09, applying Density Functional Theory (DFT) at the B3LYP level. The basis set of 6-31G* was used in the calculations (Supercomputation Service of UCLM).

2. H NMR, ^{13}C NMR, FT-IR and MALDI-TOF spectra

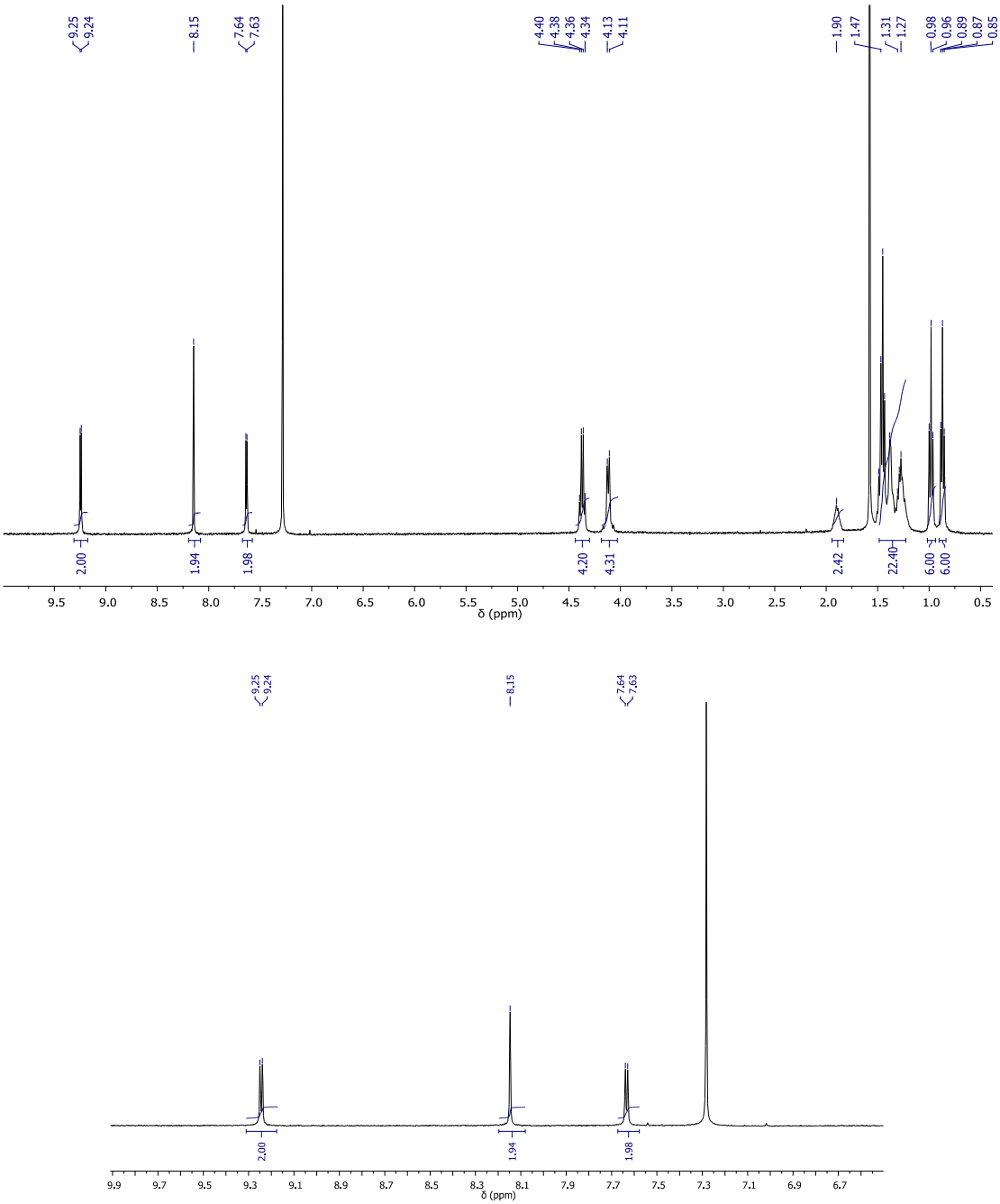

Fig. S1. ^{1}H NMR of **MPU2** (400 MHz, $CDCl_3$).

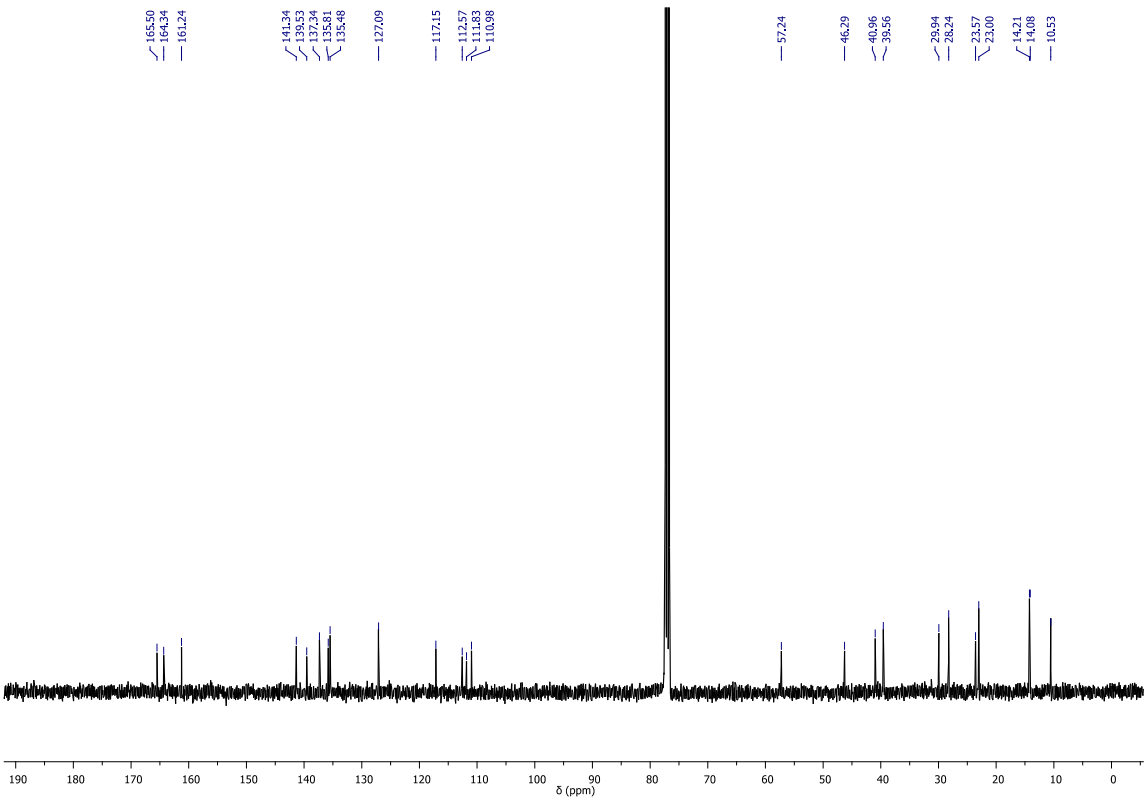

Fig. S2. ^{13}C NMR of compound **MPU2** (100 MHz, $CDCl_3$).

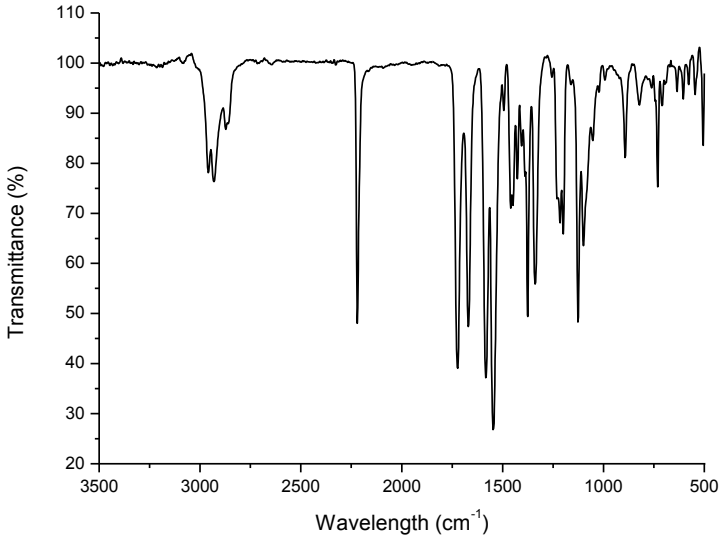

Fig. S3. FT-IR (KBr) of compound **MPU2**.

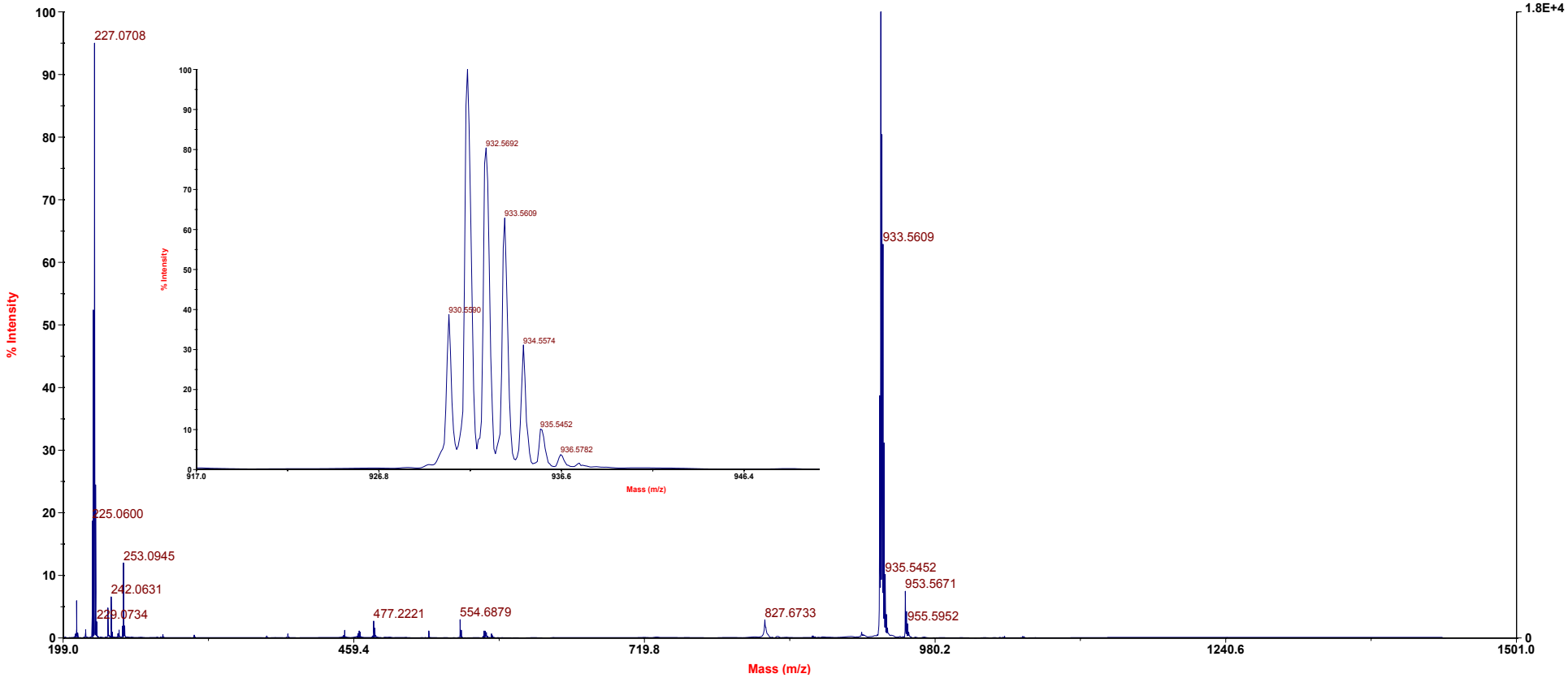

Fig. S4. MALDI-TOF MS spectrum of compound **MPU2** (Matrix: Dithranol).

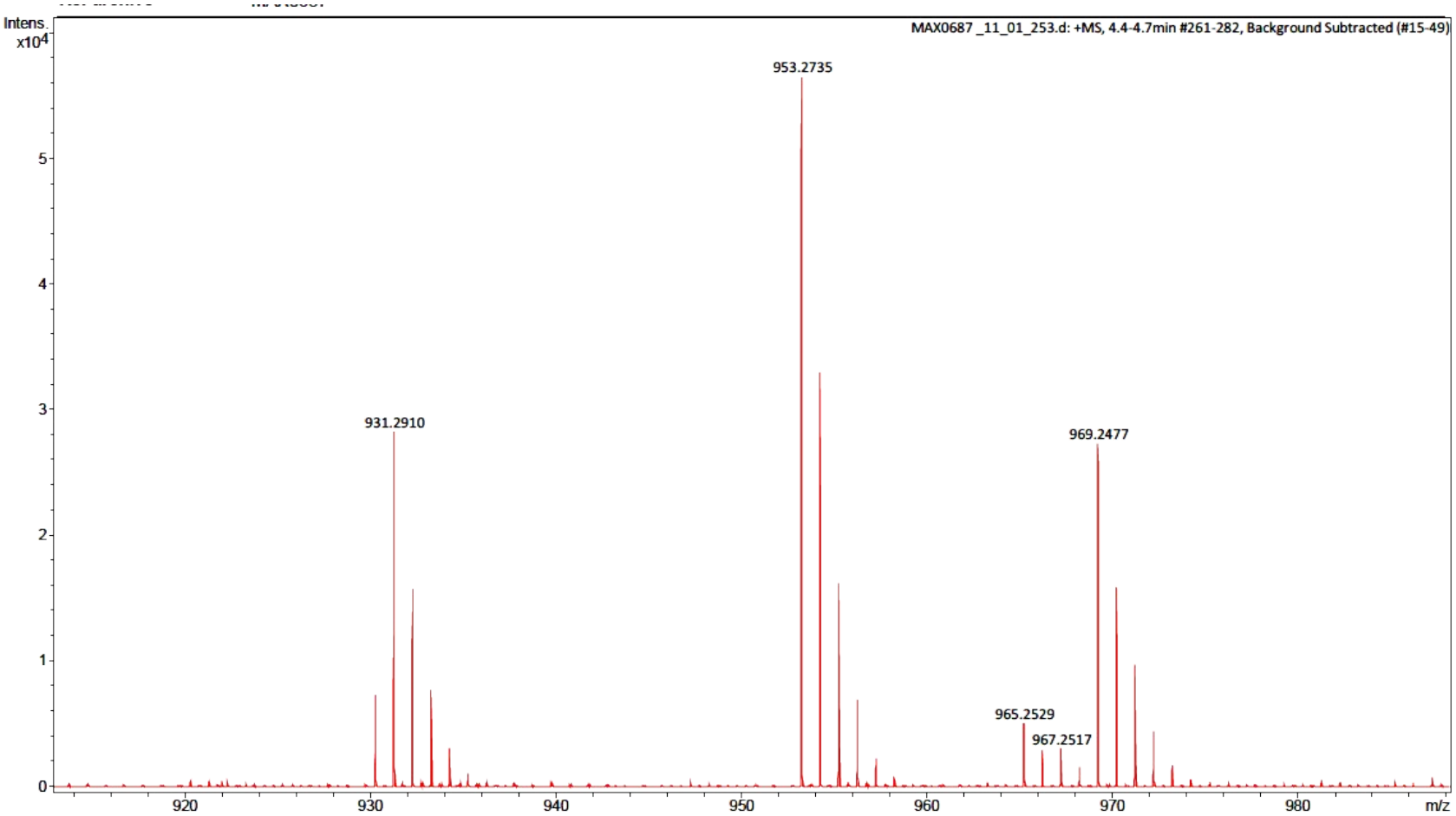
Intens.
x10^4
MAX0687 _11_01_253.d: +MS, 4.4-4.7min #261-282, Background Subtracted (#15-49)
953.2735
931.2910
969.2477
965.2529
967.2517
5
4
3
2
1
0
920
930
940
950
960
970
980
m/z

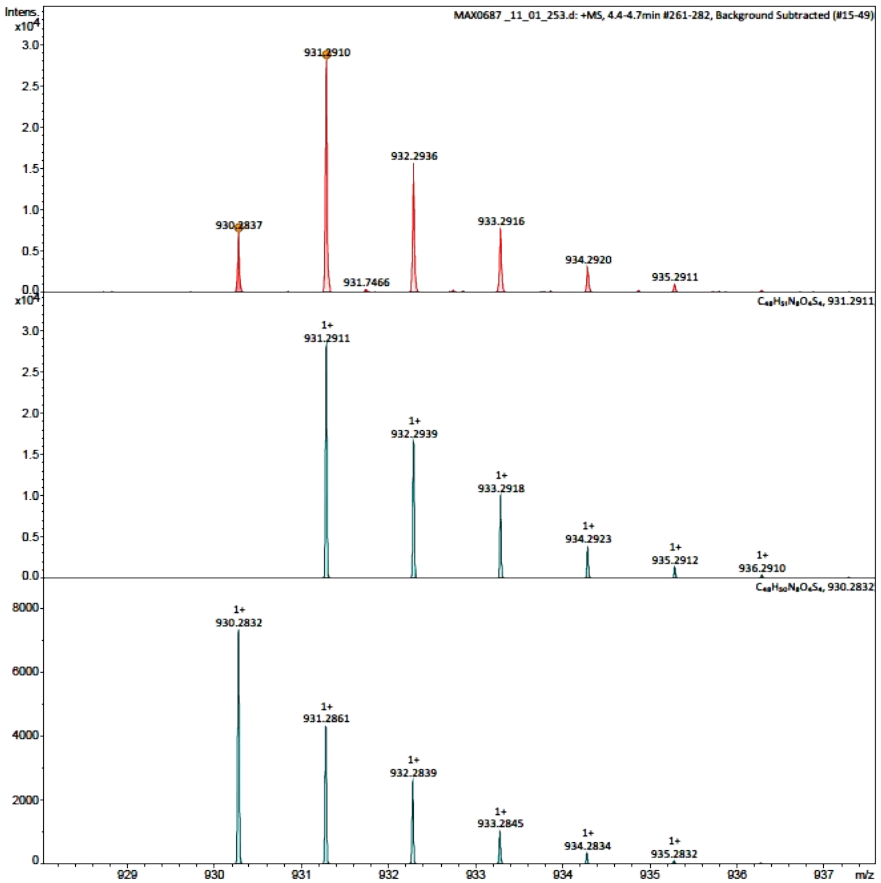
MAX0687 _11_01_253.d: +MS, 4.4-4.7min #261-282, Background Subtracted (#15-49)
Intens.
x10^4
931.2910
932.2936
930.2837
933.2916
934.2920
935.2911
931.7466
C48H51N4O4S4, 931.2911
1+ 931.2911
1+ 932.2939
1+ 933.2918
1+ 934.2923
1+ 935.2912
1+ 936.2910
C48H50N4O4S4, 930.2832
1+ 930.2832
1+ 931.2861
1+ 932.2839
1+ 933.2845
1+ 934.2834
1+ 935.2832
m/z

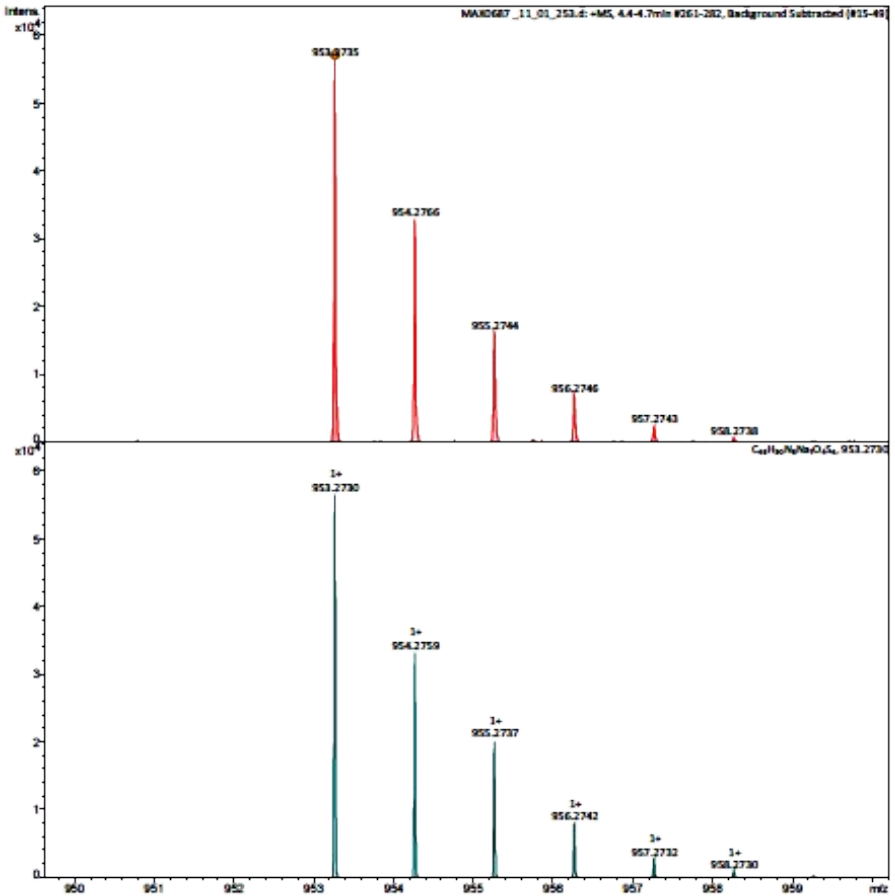
MAX0687 _11_01_253.d: +MS, 4.4-4.7min #261-282, Background Subtracted (#15-49)
Intens.
x10^4
953.2735
954.2766
955.2744
956.2746
957.2743
958.2738
C48H50N4Na2O4S4, 953.2730
1+ 953.2730
1+ 954.2759
1+ 955.2737
1+ 956.2742
1+ 957.2732
1+ 958.2730
m/z

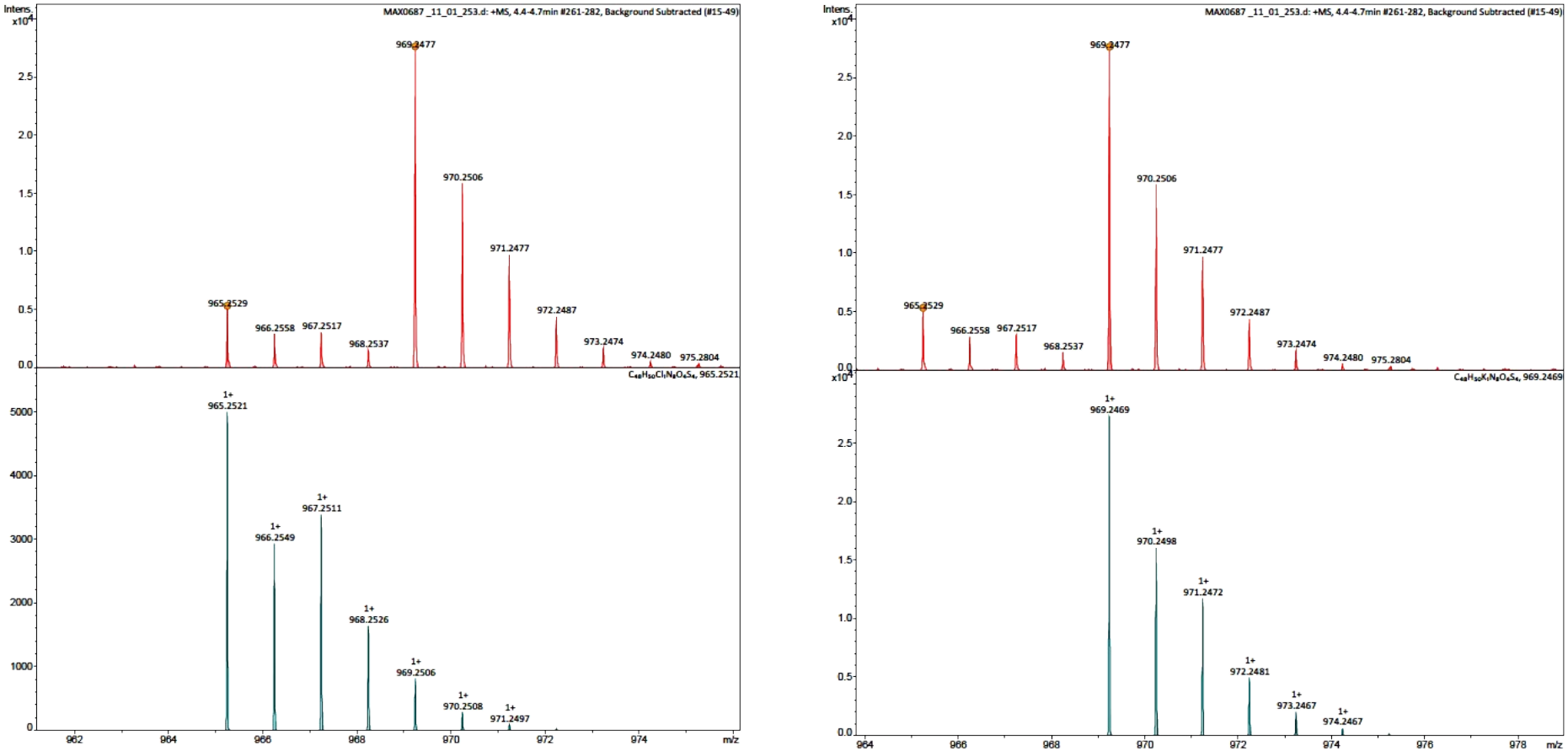

Fig S5. ESI Positive HR-MS spectrum and isotopic distributions of MPU2 (+1ml of CH_2Cl_2; Diluted from 100 ul to 1000 ul with Acetonitrile+0.1% Formic acid)

3. TGA-DSC thermogravimetric analysis compound MPU2

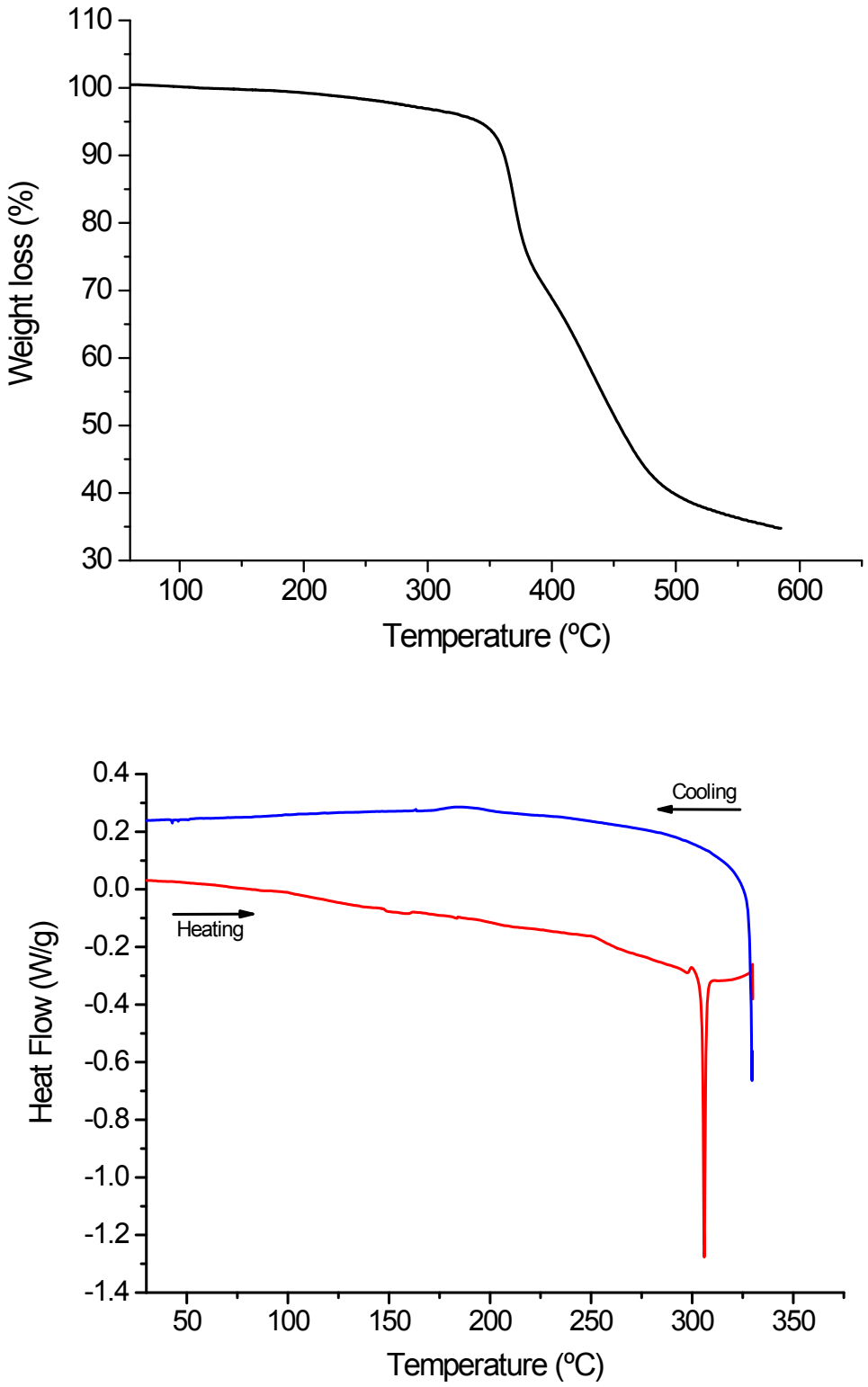

Fig. S6. TGA (top) and DSC (bottom) curves of **MPU1**

4. Theoretical calculations

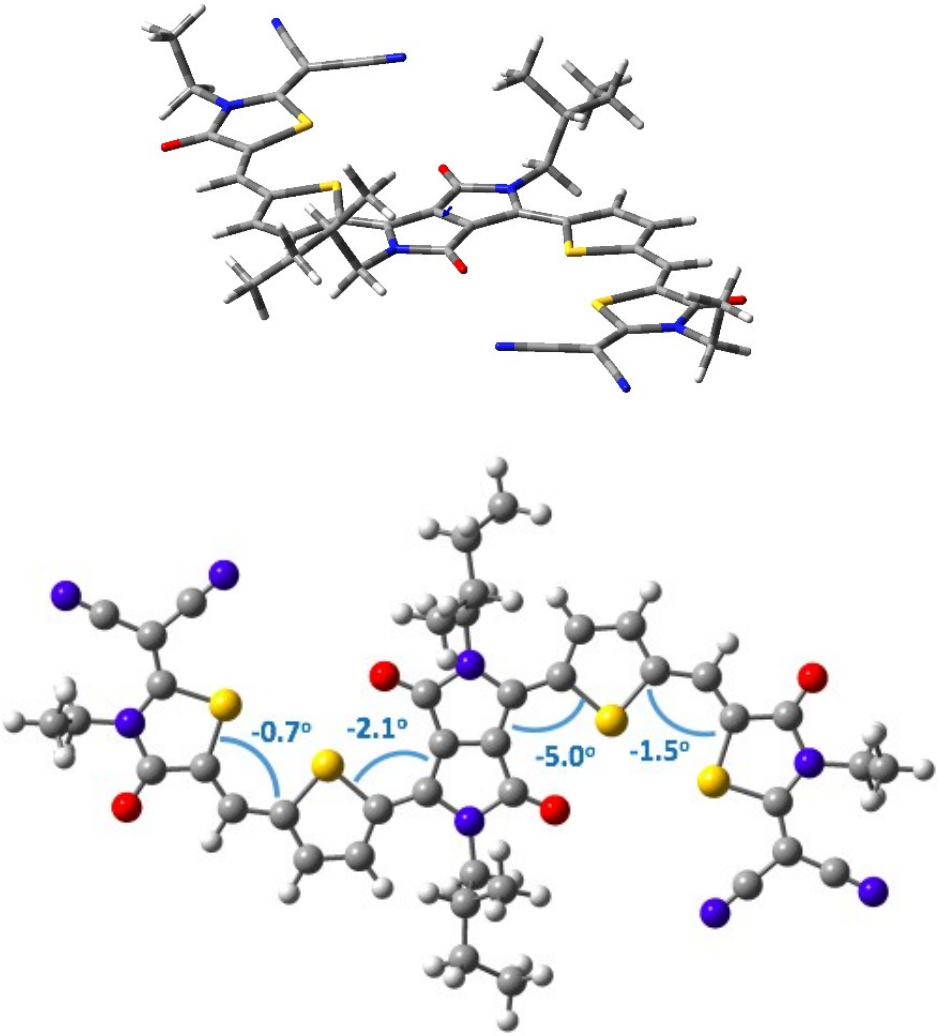

Fig. S7. Geometry optimized by theoretical calculations (Gaussian 09W, DFT-B3LYP 6-31G*) of compound **MPU2** (top) and its most important dihedral angles (bottom).

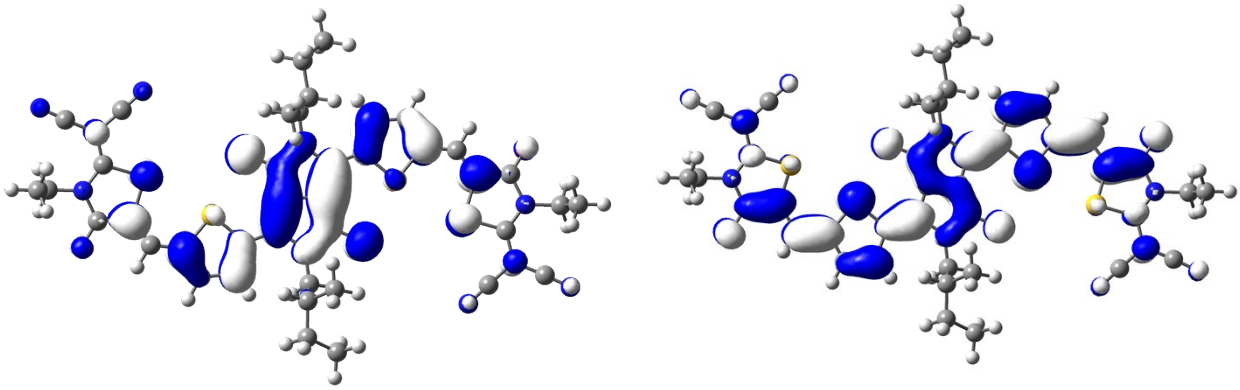

HOMO: -5.65 eV LUMO: -3.83 eV

Fig. S8. Isovalue contours and energies calculated for the frontier molecular orbitals of **MPU2**

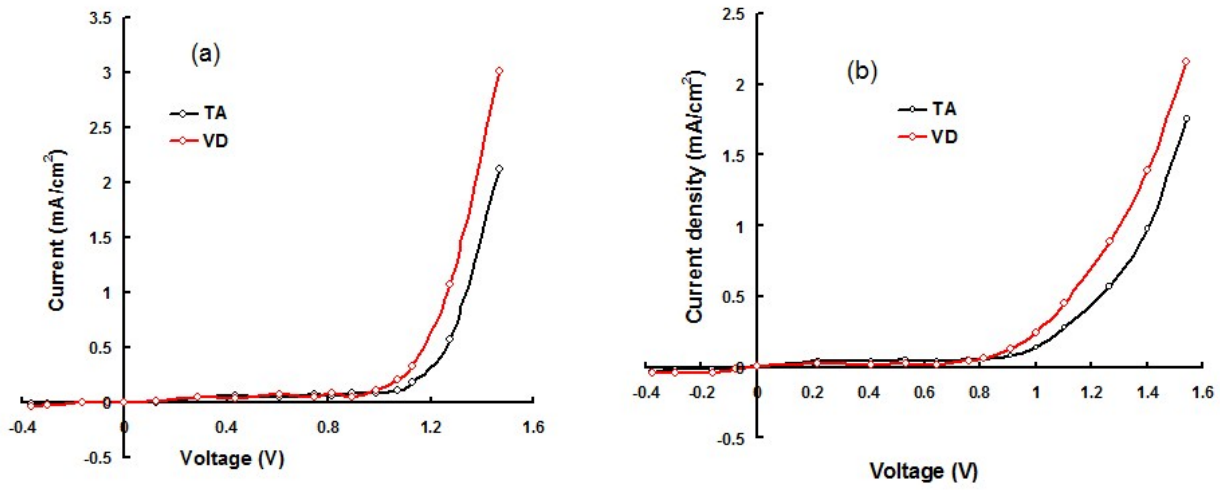

Fig. S9. Dark J-V characteristics of devices optimized (a) **MPU1**:DTS(QxHTh$_2$)$_2$ and (a) **MPU2**:DTS(QxHTh$_2$)$_2$ active layers processed with thermal annealing (TA) and vacuum drying (VD)

Table S1. Photovoltaic parameters of DTS(QxHTh$_2$)$_2$:**MPU1** and DTS(QxHTh$_2$)$_2$:**MPU2** based devices with (1:2 weight ratio) proceesed with CF and DIO/CF solutions, using DTS(QxHTh$_2$)$_2$ as donor

Acceptor	J_{sc} (mA/cm^2)	V_{oc} (V)	FF	PCE (%)	PCE (%)[c]
MPU1[a]	5.23	1.04	0.34	1.85	1.79
MPU2[a]	6.12	0.97	0.37	2.20	2.15
MPU1[b]	7.12	1.02	0.51	3.70	3.64

[a]cast from CF
[b](3v%)/CF
[c]average of 8 devices